JOURNAL OF MATERIALS SCIENCE 16 (1981) 1843–1852

Craze intersections in biaxially-stressed polystyrene

PAUL S. KING, EDWARD J. KRAMER
Department of Materials Science and Engineering, and the Materials Science Center, Cornell University, Ithaca, New York 14853, USA

Crazes are produced on two orthogonal planes in both thin film and macroscopic samples of polystyrene by sequentially applying two orthogonal tensile strains ϵ_1 and ϵ_2. Although many crazes produced by the second strain ϵ_2 (secondary crazes) are stopped when they meet a primary craze, some intersections occur. The fraction of craze meetings resulting in intersection increases from 20% at $\epsilon_1 = \epsilon_2 = 3\%$ to 55% at $\epsilon_1 = \epsilon_2 = 5\%$; intersections also occur preferentially in thin regions of primary crazes. The craze fibril structure in the intersection has a much lower fibril volume fraction, v_f, than either of the two crazes from which it formed. The fibril volume fraction in the intersection is approximately given by the product of the fibril volume fractions of the two crazes, in agreement with a prediction based on the surface drawing mechanism of craze thickening. At higher strain levels the v_fs of the intersections are lower, leading to higher fibril stresses and enhanced fibril fracture; an increasing fraction of intersections breaks down to form large voids at these higher strain levels. Fractography of macroscopic samples containing intersecting crazes demonstrates that voids formed at the intersections can act as nuclei for cracks causing premature fracture of the material.

1. Introduction

In response to a tensile stress, glassy polymers can exhibit crazing, a unique mode of localized plastic deformation. Crazes are thin planar zones of cavitation, which develop perpendicular to the maximum principal stress. The craze microstructure consists of an interconnected void network bridged by an array of tiny fibrils which give the craze significant load-bearing capability. Although often mistaken for cracks which they resemble optically, crazes are not cracks mechanically. However, it is now well established that when cracks initiate in these materials, they usually form within a craze which has previously grown under the applied stress [1–7]. This crack initiation process involves the breakdown of the fibril structure of the craze to form small voids which then expand slowly (more rapidly as they become larger) to become cracks. The early stages of void and crack growth within the craze usually take place in the "midrib", a central slab ~ 80 nm thick, which has a lower volume fraction of fibrils than the outer layers of the craze. It seems logical that the initial fibril failure should occur in this region since the true tensile stress in the fibrils is highest here. Beyond these conjectures there is little known about the initial stages of fibril failure which give rise to these voids. Clearly, however, any event which hastens fibril breakdown (or which produces relatively large voids within the crazes) is a potential cause of premature polymer failure.

In this paper we demonstrate that craze intersection is a cause of premature fibril breakdown. When two crazes intersect each other, the region of the intersection has a much lower fibril volume fraction than either of the crazes. At high stress levels the intersection region is readily converted into a long (cylindrical) void which can expand rapidly to produce final failure of the craze.

2. Experimental methods

Polystyrene (PS) films, 0.4 to 0.6 μm in thickness, were prepared by drawing glass microscope slides

0022–2461/81/071843–10$03.00/0

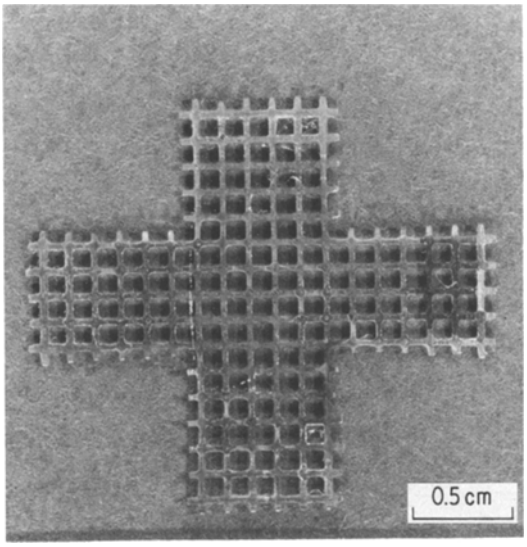

Figure 1 Cross-shaped copper grid configuration used for biaxial strain experiments.

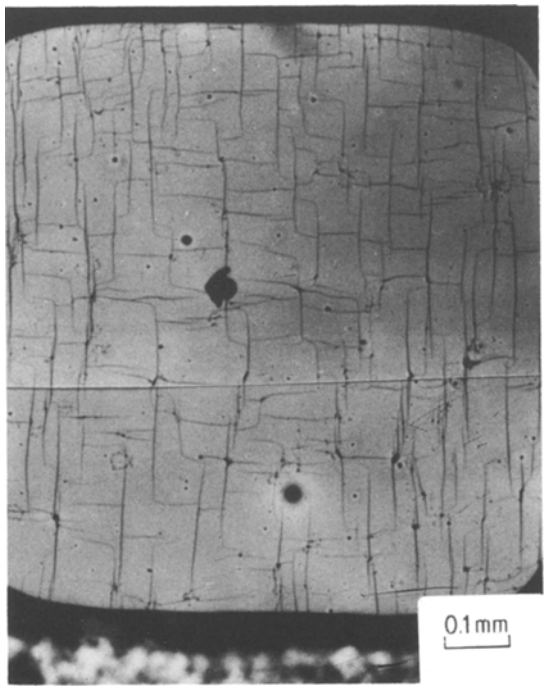

Figure 2 Optical micrograph of the PS film over a typical grid square showing intersecting crazes.

from a solution of PS ($\bar{M}_W$ = 264 600 and $\bar{M}_N$ = 110 300) in toluene. The polystyrene did not contain mineral oil, commonly added to commercial PS as a processing aid. Film thicknesses were measured using a Zeiss interference microscope.

Ductile copper grids were cut into the cross-shaped configuration shown in Fig. 1. The grid cross has a central area 6 mm × 6 mm square which can be strained in either of two orthogonal directions by pulling the appropriate arms of the cross. A dilute solution of PS in toluene was used to coat the grid, ultimately to act as a bonding agent between the film and the grid.

The PS film was floated off the glass slide on to the surface of a water bath, to which a few drops of ethanol had been added (to reduce surface tension). The film was subsequently picked up on the centre of the copper grid cross and, after drying in air to remove water, was exposed to toluene vapour for 2 min. The vapour swells and softens the PS film and the coating on the grid bars just enough so that a good bond is formed between film and grid.

After drying the bonded film for 24 h to remove toluene, the copper grid cross was fastened to a small strain frame and extended in tension along one direction of the cross. The strain applied to the copper grid is permanent (the grid deforms plastically) and thus holds the PS film under the desired tensile strain ϵ_1. After any crazes which formed had reached their equilibrium length, the grid was rotated 90° and the other arm of the cross was strained in tension to a strain ϵ_2. At high enough strain levels (both $\epsilon \gtrsim 0.5\%$) a second set of crazes formed perpendicular to the first set. The film was examined under an optical microscope (Fig. 2 shows an optical micrograph of a typical grid square). Grid squares of interest could be cut from the grid using a razor blade without perturbing the strain in the film. The crazes in these films were then examined using transmission electron microscopy by means of a JEM 200 microscope operated at 200 kV.

Fibril volume fractions v_f of the crazes and their intersections were determined by microdensitometry of electron image plates [8, 9]. The optical densities, ϕ, of areas of the plate corresponding to a hole, the solid film and the craze, were used to determine v_f according to the equation [9],

$$v_f = 1 - \frac{\ln(\phi_{craze}/\phi_{film})}{\ln(\phi_{hole}/\phi_{film})}. \quad (1)$$

Care was taken to maintain the exposure of the plate within the linear response region of its sensitivity curve.

Macroscopic fracture tests were also conducted

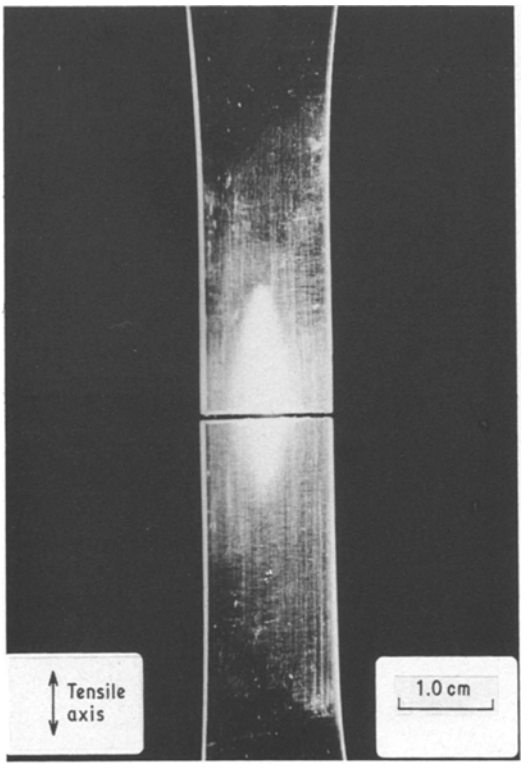

Figure 3 Specimen pulled to fracture in macroscopic tensile fracture experiments. It has been precrazed (white area) with precrazes lying parallel to the tensile axis.

on specimens with intersecting sets of crazes. Tensile test specimens of the standard ASTM shaped shown in Fig. 3 were machined from 0.72 mm thick PS sheet. The edges of the specimen were carefully polished with 600 grit SiC paper to remove any machining marks that would act as stress concentrations and thus as a starting point for crazes and cracks. The tensile specimens were bent around a cylinder of radius ρ that was held parallel to the long axis of the specimen. This bending produced a tensile strain ϵ_{max} at the outer surface of the specimen of

$$\epsilon_{max} = \frac{T}{2\rho + T}, \qquad (2)$$

where T is the specimen thickness. Crazes were produced parallel to the long axis of the specimen on the outer surface (furthest from the cylinder) using this technique. By repeating the bending with the opposite broad surface bent against the cylinder, crazes parallel to the long axis of the specimen could be generated on both surfaces. Specimens were then pulled in tension to failure at an extension rate of 0.0508 mm min^{-1}. The fracture surfaces of these pre-crazed specimens were compared using optical and scanning electron microscopy with those of specimens that had no precrazes running parallel to the tensile axis (and thus no possibility of craze intersection).

3. Results and discussion

3.1. Intersecting craze morphology.

Fig. 4 shows a typical craze morphology produced by sequential strains ϵ_1 and ϵ_2 applied to the grid in the two orthogonal directions. A primary craze, produced by ϵ_1, running horizontally in the figure is intersected by a craze growing vertically due to the final strain, ϵ_2. A second craze, growing vertically has been stopped by the primary craze.

While this craze morphology is typical of that produced when sufficient time is allowed for crazes to attain their final length under ϵ_1, a different morphology is seen if the second strain is applied while the primary crazes are still growing. As illustrated in Fig. 5, crazes which turn by $\sim 90°$ are produced if the second strain is applied too soon. The reason for this behaviour seems clear. If the primary craze is still growing, it will change direction to follow the plane of maximum principal stress which is changing as a result of the increasing ϵ_2 (ϵ_2 cannot be increased instantaneously). As a result, when ϵ_2 reaches its final value, the craze tip has turned through almost a right angle and now grows on a plane approximately perpendicular to ϵ_2. If the primary crazes have stopped growing, they apparently do not resume growth on application of ϵ_2; instead new crazes nucleate and grow on planes perpendicular to ϵ_2, eventually producing intersections of the type shown in Fig. 4.

As also shown in Fig. 4, the secondary crazes (produced by ϵ_2) are often stopped by primary crazes. The craze-stopping role of primary crazes has also been observed previously by Beahan *et al.* [5]. Fig. 6 shows a high-magnification view of a secondary craze tip stopped at a primary craze. The opening displacement of the secondary craze has split the fibril structure of the primary craze. Within the primary craze the secondary craze is bridged only by a few major fibrils of the primary craze running principally diagonally and the so-called tie fibrils between major fibrils. The lower load-bearing capacity of the rarified fibril structure in this region is evidenced by the larger craze displacements (in the ϵ_2 direction) here. The

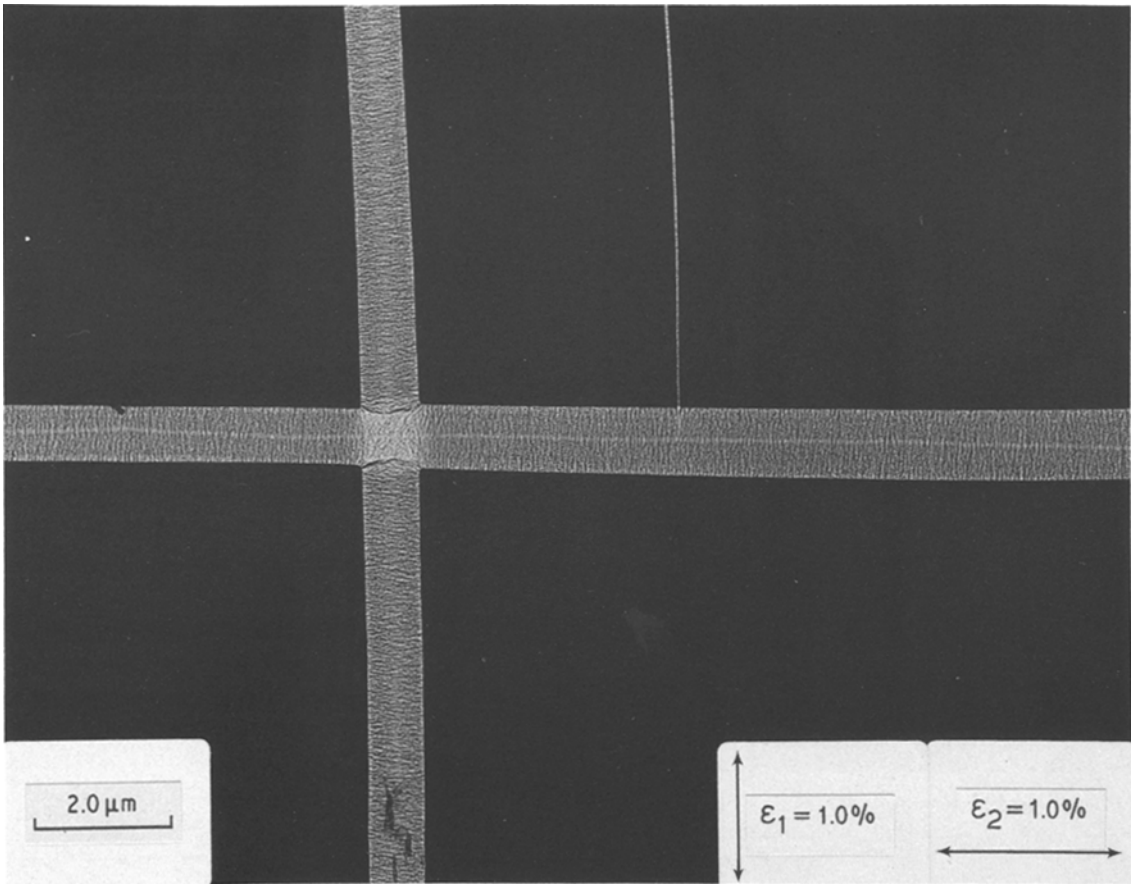

Figure 4 Transmission electron micrograph of intersecting crazes in a typical grid square. $\epsilon_1 = 1\%$ and $\epsilon_2 = 1\%$.

lateral weakness of the fibril structure of the primary craze also means that the stress concentration which existed at the tip of the secondary craze when it hit the primary craze is transferred only very inefficiently to the opposite side of the primary craze where the tip of the secondary craze must be renucleated if a fully-fledged intersection is to occur. One would, therefore, expect that secondary crazes are more often stopped by thicker portions of the primary crazes and this expectation is borne out by experiment. It is observed that most craze intersections occur where the primary craze is thin (see Figs 7 and 11) whereas secondary crazes are often stopped by thick regions of the primary craze. Whereas the lateral weakness of the primary craze might prevent intersection at low ϵ_2, at higher ϵ_2 one might expect the load transfer across the primary craze to assume less importance. Indeed whereas we observe that only 20% of the secondary craze–primary craze "meetings" produced intersections at $\epsilon_2 = 3\%$ (80% of the secondary crazes were stopped at primary crazes), some 43% of orthogonal craze meetings produced intersections if the ϵ_2 applied was 4.5%, and 55% of orthogonal craze meetings produced intersections if ϵ_2 was 5.0%.

3.2. Craze intersection microstructure

The microstructure of a typical craze intersection produced at low orthogonal strain ($\epsilon_1 = \epsilon_2 = 1\%$) is shown in Fig. 7. The fibril volume fraction in the intersection is obviously lower than that in either the primary or secondary crazes. The predominant fibril direction in the intersection is approximately parallel to ϵ_1, i.e. parallel to the major fibril direction in the primary craze, although many tie fibrils running at other directions between these major fibrils are observed. It is as if the displacements produced by the secondary craze have simply separated the fibrils of the primary craze. This fibril separation is exactly what one would expect to be produced by the surface-drawing mechanism of thickening of the

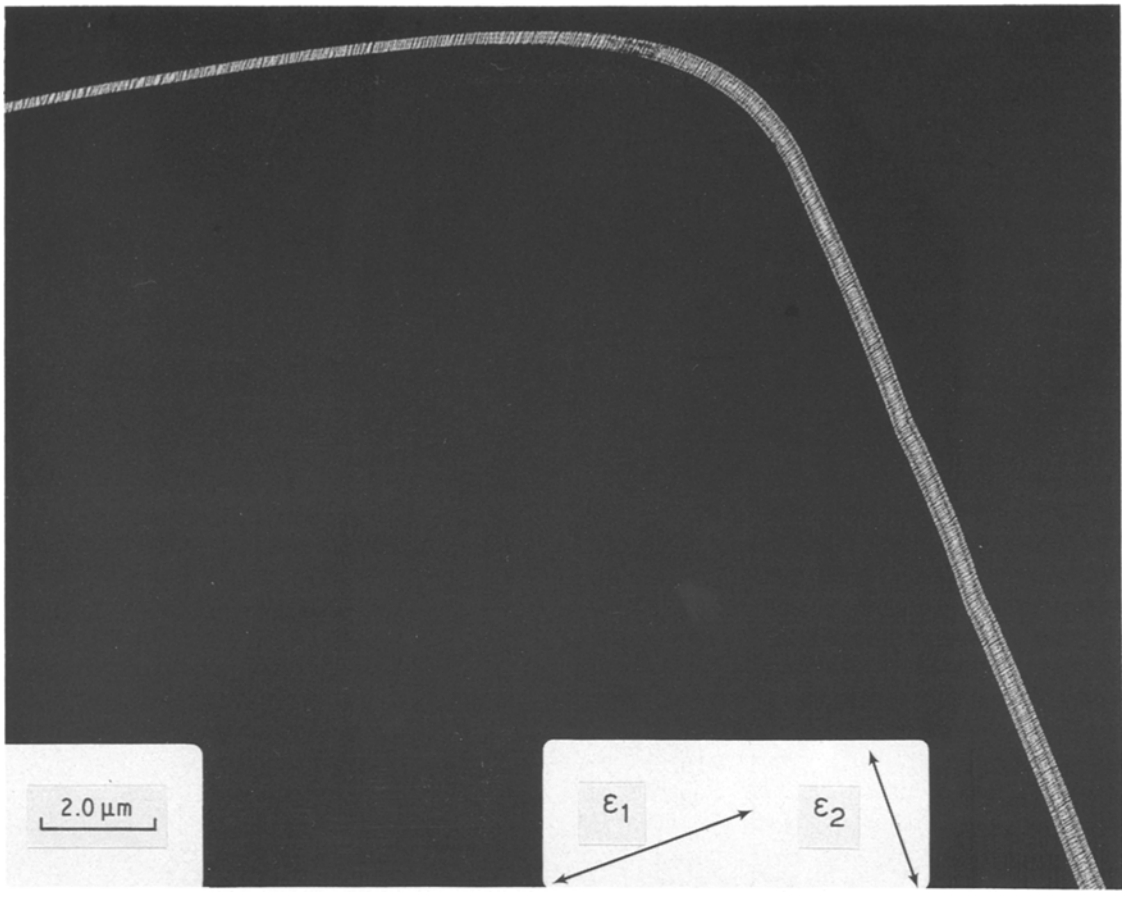

Figure 5 Transmission electron micrographs of a "bent" craze produced by applying the second strain ϵ_2 while the primary craze was still growing.

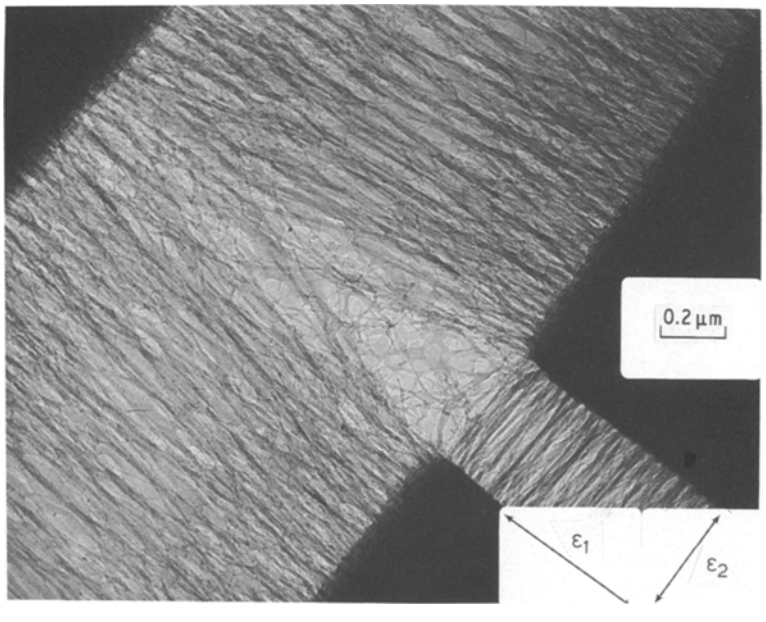

Figure 6 Transmission electron micrograph of a secondary craze tip stopped by a primary craze.

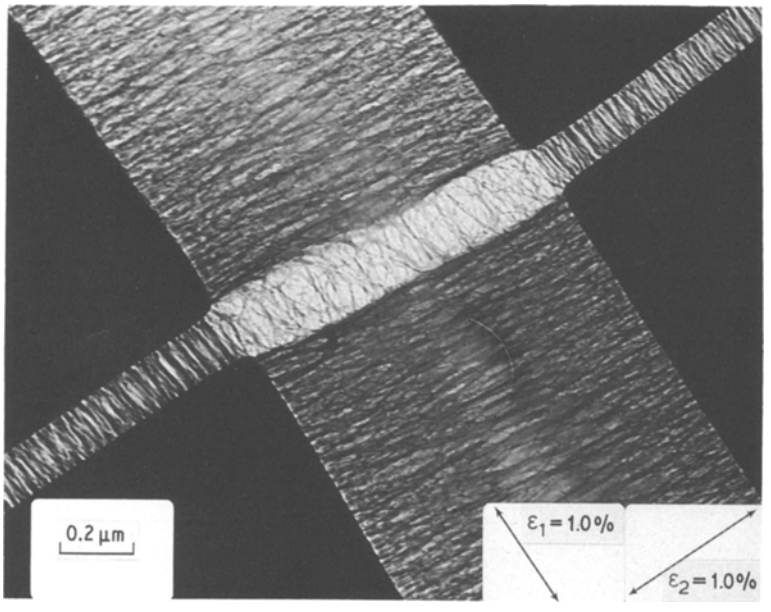

Figure 7 Transmission electron micrograph of the fibrillar microstructure of a typical craze intersection produced by $\epsilon_1 = 1\%$ and $\epsilon_2 = 1\%$.

secondary craze. It has been previously established that air crazes in PS thicken by drawing more polymer into the craze fibrils from the craze surfaces [9] rather than by fibril creep. If the secondary craze thickens by such a mechanism one would expect to observe that the major fibril spacing in the primary craze would increase by a factor λ_2, where λ_2 is the extension ratio of fibrils in the secondary craze, as the polymer at the primary craze boundary is drawn into secondary craze fibrils parallel to that boundary. If fibril creep were the mechanism of secondary craze thickening one would expect to see few fibrils from the primary craze in the intersection region.

One can make this hypothesis more quantitative by observing that if the fibril volume fraction is v_{f1} in the primary craze, and if the major fibril separation in the intersection is increased by $\lambda_2 = 1/v_{f2}$ where v_{f2} is the volume fraction of fibrils in the secondary craze, the volume fraction of fibrils in the intersection region should be given by

$$(v_f)_{int} = v_{f1} \cdot v_{f2}. \quad (3)$$

This relation can be tested quantitatively since the fibril volume fractions can be measured by microdensitometry of the electron image plates. Before such quantitative comparisons can be made, however, one must correct for the effects of a groove that has been shown to form where the craze intersects the film surface [10]. The geometry of this groove is shown in Fig. 8. Typically the depth of the groove is about 50 nm. Because of the surface groove, the actual volume fraction of fibrils in the craze in a thin film is larger than that measured, i.e.

$$(v_f)_{actual} = (v_f)_{measured} \left(1 - \frac{2t_s}{t}\right)^{-1}, \quad (4)$$

where t is the thickness of the film and t_s is the depth of the surface groove. For our films which are ~ 550 nm thick, the correction produces an increase of about 22% in the fibril volume fraction. In making the comparison the measured values of $(v_f)_1$, $(v_f)_2$ and $(v_f)_{int}$ were all increased by a factor of 1.22.

Fig. 9 shows a test of the hypothesis. In this figure the fibril volume fraction in the intersection is plotted versus the product of the fibril volume fractions of the two intersecting crazes. Despite

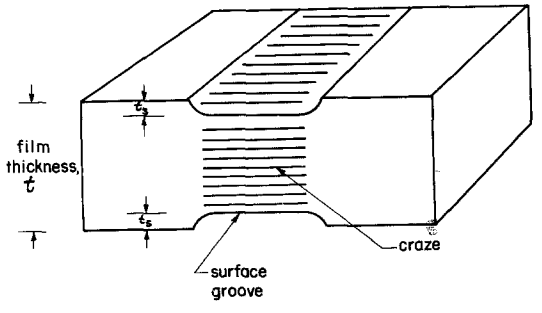

Figure 8 Schematic view of craze microstructure through the thickness of the film showing the surface groove.

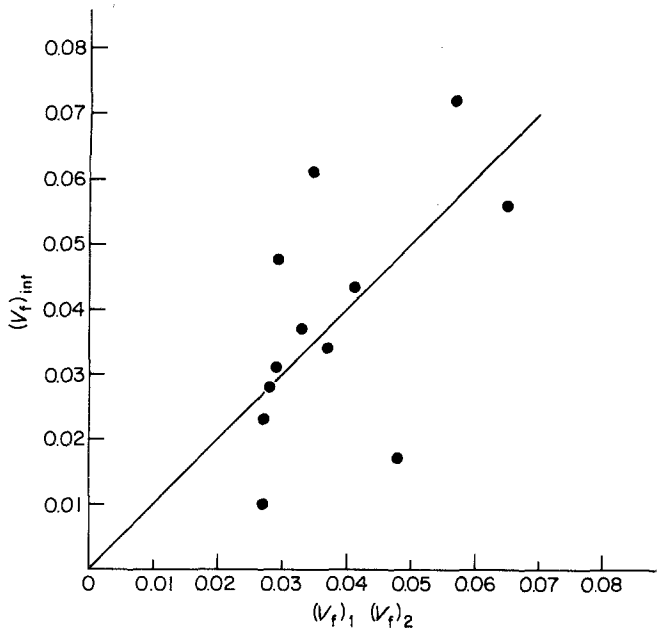

Figure 9 Craze fibril volume fraction observed in intersections plotted against the product of the fibril volume fractions of the individual crazes. All fibril volume fractions have been corrected for the presence of the surface groove by multiplying by a factor of 1.22.

the large scatter in the data, the correlation observed is quite strong. However, a number of craze intersections, particularly those produced at higher strains, have lower v_fs than predicted. Table I shows the fibril volume fractions of both the primary and secondary crazes and their intersections at several applied strain levels ($\epsilon_1 = \epsilon_2$ in these experiments). Each entry represents the average of measurements on about five intersections. Whereas the v_f of the primary and secondary crazes decreases only slightly with increasing strain, the v_f of their intersection decreases markedly.

It seems reasonable to attribute these results to the breakdown of craze fibrils in the intersections due to the higher fibril stresses there. Since the true fibril stresses in the intersection are approximately $\sigma/(v_f)_{int}$ where σ is either of the biaxial tensile stresses in the film, the very small values of $(v_f)_{int}$ imply large fibril stress that might logically lead to increased fibril failure. Comparing the microstructure of intersections at higher strain levels ($\epsilon_1 = \epsilon_2 = 3\%$) as seen in Fig. 10 with those produced at lower strain levels ($\epsilon_1 = \epsilon_2 = 1\%$) as seen in Fig. 7, one has the qualitative impression that there are very few fibrils left intact at the higher levels and that the fibril failure must be quite important. This impression is reinforced by the fact that at higher biaxial strain levels no fibrils could be observed in many of the craze intersections; they had broken down to form large voids. Fig. 11 shows such an intersection in a film stretched to $\epsilon_1 = \epsilon_2 = 5\%$. At this strain level approximately 20% of the craze intersections were voids. At higher strain levels film fracture occurs with the cracks presumably originating at such intersections.

3.3. Macroscopic fracture experiments

The preceding thin-film results make it appear likely that craze intersections can breakdown to form large voids and thus act as initiators of cracks in the material. To check this hypothesis we have carried out macroscopic fracture experiments in which tensile samples, which were precrazed on both surfaces with the crazes running parallel to the tensile axis, were pulled to fracture. The precrazed region, which was produced by a surface strain ϵ_{max} of 3%, covered only about $\frac{1}{4}$ of the gauge section. When the samples were

TABLE I Fibril volume fraction of primary and secondary crazes and their intersections

Biaxial strain	v_f primary craze	v_f secondary craze	v_f intersection
$\epsilon_1 = \epsilon_2 = 1.0\%$	0.17	0.22	0.046
$\epsilon_1 = \epsilon_2 = 2.0\%$	0.18	0.21	0.037
$\epsilon_1 = \epsilon_2 = 3.0\%$	0.17	0.16	0.024

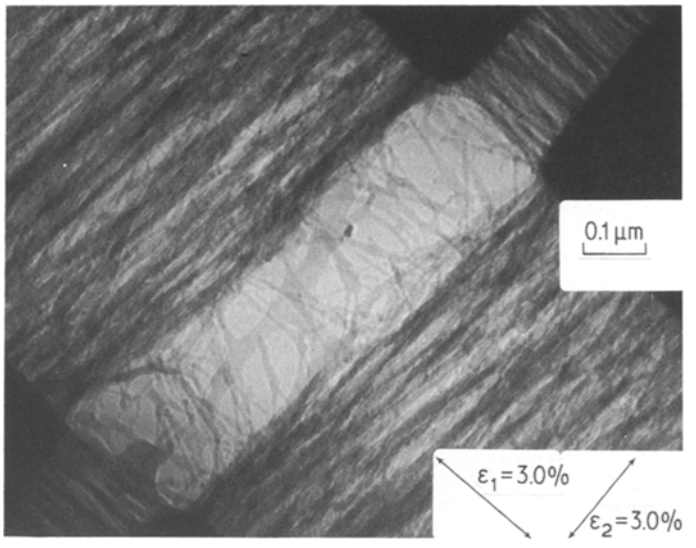

Figure 10 Transmission electron micrograph of a typical craze intersection produced by $\epsilon_1 = \epsilon_2 = 3\%$.

extended in tension a second set of crazes originated perpendicular to the tensile axis prior to fracture. Unfortunately, owing to non-uniformities in specimen shape and loading, the second set of crazes did not always form uniformly along the gauge section and did not always intersect the other set of crazes. In those cases where intersection did occur, the crack which produced the final fracture always originated in the region of intersection of the two sets of crazes. Since in many of these experiments the number of crazes perpendicular to the tensile axis was much greater outside the area where the two sets of crazes intersected, this result strongly implies that the craze interactions act as preferential crack "nuclei".

Final confirmation of this hypothesis comes from fractographic evidence. Fig. 12 shows an optical micrograph of the fracture origin in a PS specimen that had not been precrazed parallel to the tensile axis. This micrograph is similar to those published by Murray and Hull [2, 4] and shows a surface mirror region where the crack grew in the centre of the craze and intersected secondary voids that had nucleated at various other positions in the craze. An elliptical region of intersection around such a secondary void is marked at A. The outline of the secondary void/crack is seen because the last layer of craze fibrils to fracture as the primary crack and secondary void met is highly deformed. One might expect to be able to identify any secondary voids which grew from craze intersections by similar fracture-surface markings.

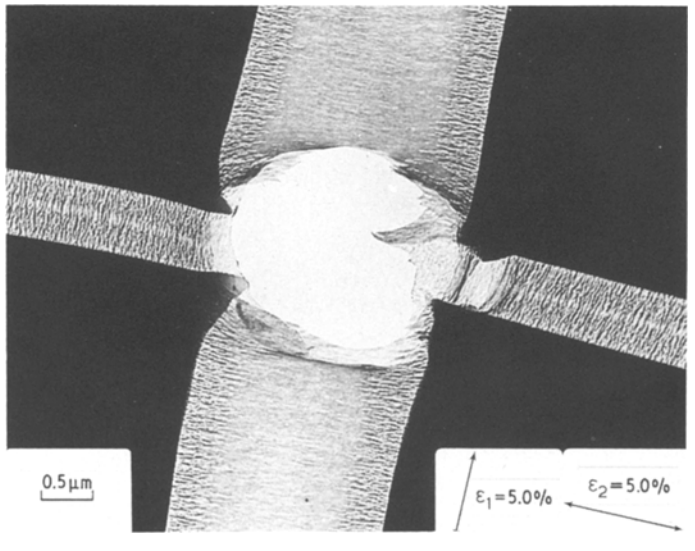

Figure 11 Transmission electron micrograph of a craze intersection produced of $\epsilon_1 = \epsilon_2 = 5\%$ in which the fibril structure has broken down to form a void.

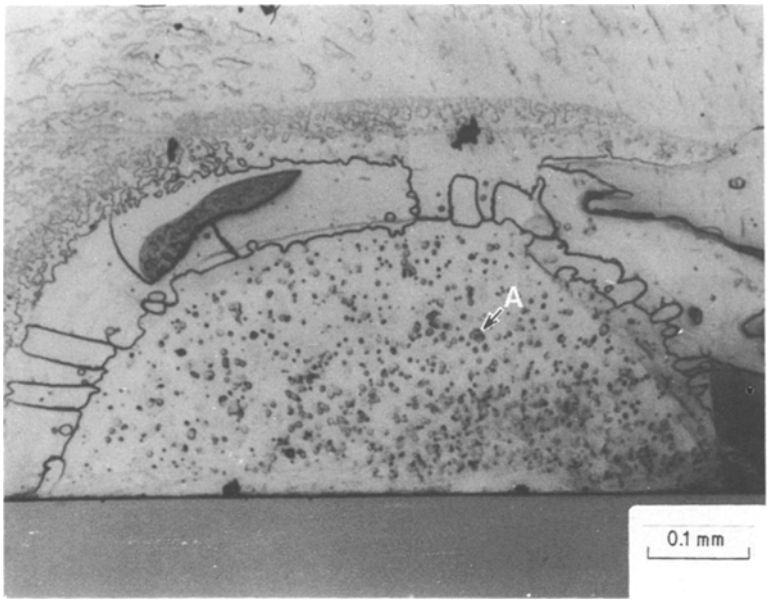

Figure 12 Optical micrograph of the fracture surface around the origin of fracture of a PS specimen that was not precrazed prior to fracture. Note secondary fracture at A where a void growing in the craze met the main crack.

Fig. 13 shows an optical micrograph of the fracture origin on the fracture surface of a PS specimen in which the fracture originated in the region of intersecting crazes. The crazes parallel to the tensile axis are apparent as a set of parallel lines normal to the specimen surface. A detailed analysis of the fracture surface using the principles outlined by Murray and Hull shows that the fracture originated somewhere in the region A. Many of the craze intersections in this region show "ridges" well outside and approximately parallel to the intersection. A region within region A was examined at higher magnification using the scanning electron microscope. Fig. 14 shows a micrograph of this region. The "ridges" that surround many of the craze intersections are clearly visible as are some normal secondary fracture features (the secondary void/crack intersections). It seems clear that the ridges are secondary fracture features where long secondary voids, growing from craze intersections, were met by the main crack front. By using the topology of these, as well as that of the normal secondary features, one can locate the origin of the fracture as the craze inter-

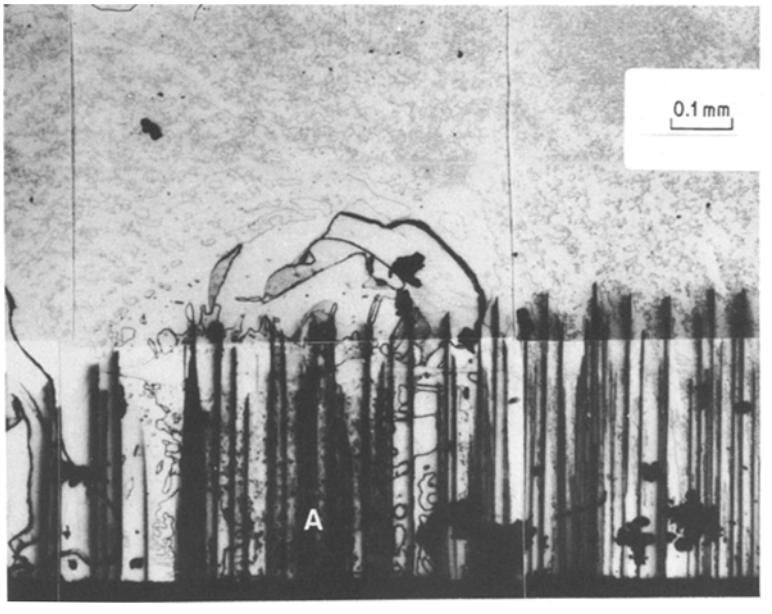

Figure 13 Optical micrograph of the fracture origin on the fracture surface of a PS sample for which the fracture originated in the region of intersecting crazes. Region A marks the fracture origin.

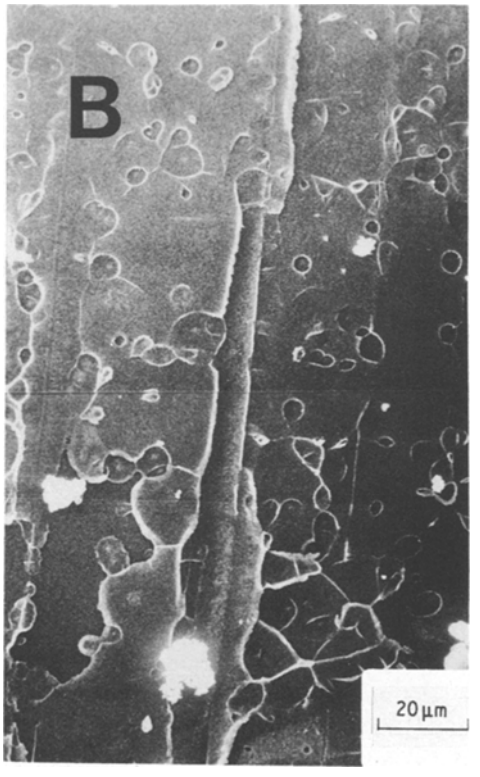

Figure 14 Scanning electron micrograph of region A in Fig. 13. Origin of fracture is at the craze intersection at B. Note "ridges" where secondary voids growing from the intersecting crazes met the growing crack front.

section marked B. Similar observations were made on other samples where the two sets of crazes intersected. It seems clear, therefore, that the preferential craze breakdown to form voids observed at craze intersection in thin films also occurs in bulk samples and can result in crack nucleation and premature fracture.

4. Conclusions

It is concluded that:

(1) when two crazes intersect, the fibril volume fraction in the intersection is approximately the product of the fibril volume fractions of the two crazes and therefore is much lower than the normal craze fibril volume fraction;

(2) the product law for the fibril volume fraction of the intersection follows directly from the surface-drawing mechanism of craze thickening;

(3) the lower fibril volume fraction results in higher fibril stresses in the intersection giving rise to more rapid fibril breakdown there to form voids. These can act as sites from which cracks develop prematurely;

(4) both craze intersection and fibril breakdown in the intersection occur more frequently at higher applied strains (and stresses);

(5) given the evidence that craze intersections can act as efficient nuclei of cracks, care should be taken to avoid stress histories which can result in formation of intersecting crazes.

Acknowledgements

The financial support of this work by the US Army Research Office at Durham through Grant no. DAAG29-79-C-0015 is gratefully acknowledged. We also benefited from the use of the facilities of the Cornell Materials Science Center which is funded by a grant from the National Science Foundation. We very much appreciate helpful discussions with our colleagues Dr Athene M. Donald, Dr Nigel R. Farrar, Vincent Wang and Michael Yaffe and especially wish to thank Dr Robert A. Bubeck of Dow Chemical Company for providing the pure polystyrene containing no mineral oil.

References

1. R. P. KAMBOUR, *J. Polymer Sci.* **4** (1966) 17.
2. J. MURRAY and D. HULL, *Polymer* **10** (1969) 451.
3. D. HULL, *J. Mater. Sci.* **5** (1970) 357.
4. J. MURRAY and D. HULL, *J. Polymer Sci. A-2* **8** (1979) 583.
5. P. BEAHAN, M. BEVIS and D. HULL, *Phil. Mag.* **24** (1971) 1267.
6. *Idem, J. Mater. Sci.* **8** (1974) 162.
7. *Idem, Proc. Roy Soc. (London)* **A343** (1975) 523.
8. H. R. BROWN, *J. Mater. Sci.* **14** (1979) 237.
9. B. D. LAUTERWASSER and E. J. KRAMER, *Phil. Mag.* **39** (1979) 469.
10. A. M. DONALD, T. CHAN and E. J. KRAMER, *J. Mater. Sci.* **16** (1981) 669.

Received 19 November and accepted 12 December 1980.